S2E SIMULATION OF AN ERL-BASED HIGH-POWER EUV-FEL SOURCE FOR LITHOGRAPHY

N. Nakamura[†], R. Kato, T. Miyajima, M. Shimada

High Energy Accelerator Research Organization (KEK), Tsukuba, Japan

T. Hotei,

The Graduate University for Advanced Studies (SOKENDAI), Tsukuba, Japan

R. Hajima,

National Institute for Quantum and Radiological Science and Technology (QST), Tokai, Japan

Abstract

Energy recovery linac (ERL) based extreme ultraviolet (EUV) free electron lasers (FELs) are candidates of a next-generation high-power EUV source for lithography. An ERL-based EUV FEL source has been designed in order to demonstrate the feasibility of generating a 10-kW class EUV power. Start-to-End (S2E) simulation including the injection beam optimization, bunch compression, FEL lasing and bunch decompression is performed for the designed EUV source. As a result it is demonstrated that the EUV FEL can produce high power more than 10 kW at 10 mA and that the electron beam can be well transported throughout the EUV source without beam loss.

INTRODUCTION

The technologies on EUV lithography are progressing based on laser-produced plasma (LPP) source [1], which is expected to produce the EUV power of 250 W or more. However it is important to develop a new-type EUV source to meet future demand for higher power than 1 kW [2]. ERL-based FELs are possible candidates of a high-power EUV source that can distribute 1 kW power to multiple scanners simultaneously. The ERLs can provide high-current and high-quality electron beams for the high-power FELs and also greatly reduce the dumped beam power and activation compared to ordinary linacs.

An EUV-FEL source based on an 800-MeV ERL has been designed using available technologies and resources to produce 10-kW class EUV power for lithography [3]. S2E simulation from the electron gun to the exit of the decelerating main linac is performed for this design to track the electron beam distribution and parameters and to evaluate the FEL performance. This paper will present results of the S2E simulation for the designed EUV-FEL source.

OVERVIEW OF EUV SOURCE

Figure 1 shows the image of the designed ERL-based EUV-FEL source [3]. In the injector design, the electron beam is generated by a 500-kV photocathode DC gun with the same structure as the 2nd gun developed for the cERL [4] and accelerated to 10.5 MeV or more by six 2-cell superconducting (SC) cavities in two cryomodules, which have the same structure as the cERL injector cavities [5]. The merger system that guides the injection beam into the recirculation loop is slightly modified from the cERL merger.

The main-linac SC cavity is a tesla-type 9-cell cavity with a large-aperture HOM-damped (higher-order-mode-damped) beam pipe. This cavity has a reduced ratio of the peak to acceleration electric fields by a factor of 1.5 compared to the cERL main-linac cavity, which is stably operated at ~8.5MV/m against the field emission [6]. Therefore stable operation at 12.5 MV/m is promising. The main linac consists of sixty-four main-linac cavities in sixteen cryomodules to accelerate the beam to 800 MeV. Quadrupole triplets are placed at every two cryomodules for beam focusing. The betatron function is optimized against beam breakup caused by the cavity HOMs and it is symmetric for acceleration and deceleration phases. After the off-crest acceleration by the main linac, the electron bunches are compressed by the 1st arc and/or a chicane down to several ten fs to increase the peak current for obtaining high FEL power and, after emitting the EUV FEL light, decompressed before the decelerating main linac by the 2nd arc. Finally they are decelerated by the main-linac cavities and dumped.
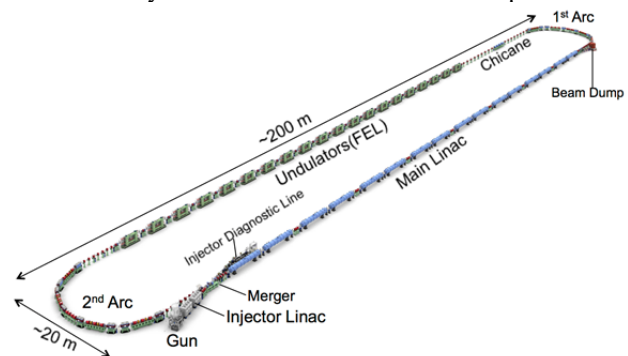

Figure 1: Image of the designed ERL-based EUV-FEL.

INJECTION BEAM OPTIMIZATION AND BUNCH COMPRESSION

The injection beam parameters from the gun to the entrance of the main linac are optimized by the tracking code *GPT* [7] and genetic algorithm. The bunch charge of 60 pC and the injection beam energy of 10.5 MeV are assumed. In addition, the bunch length at the entrance of the main linac is set to ~1 ps so that high peak current and

_____
† norio.nakamura@kek.jp

low energy spread should be ensured after the bunch compression. After optimizing the injector and merger parameters and performing the optics matching between the merger and the main linac, the vertical and horizontal normalized emittances are obtained to be 0.65 and 0.73 mm·mrad for the energy spread of 0.347 % at the entrance of the main linac.

The injection beam is accelerated off-crest by the main linac up to 800 MeV and then compressed by the 1st arc and/or a chicane to increase the peak current for obtaining high FEL power. In this S2E simulation, we use three DBA (Double-Bend Achromat) cells as the 1st arc for the bunch compression in place of two TBA (Triple-Bend Achromat) cells so far used [3]. DBA lattice has been studied to suppress coherent synchrotron radiation (CSR) effects on beams in bending sections even for a changeable bunch length [8]. The DBA optics is designed so that the betatron phase between the two bending magnets in the DBA cell is 180 degrees and two Twiss parameters at the center of the 2nd bending magnet, β_{x2} and α_{x2}, can be adjusted to optimize the horizontal emittance or performance of the bunch compression. Figure 2 shows the 1st arc optics with β_{x2}=1.0 m and α_{x2}=1.6. The bending radius and angle are 2.2 m and 30 degrees and the longitudinal dispersion of the 1st arc, R_{56}, is about 0.31 m.
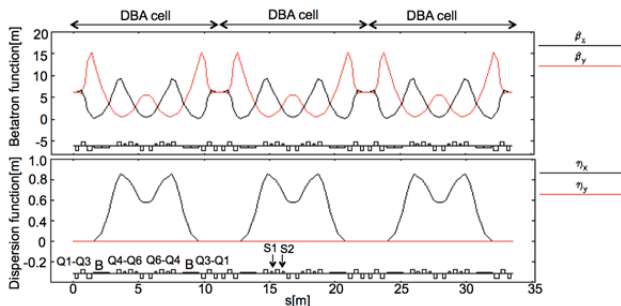

Figure 2: Betatron and dispersion functions of the 1st arc with three DBA cells having β_{x2}=1.0 m and α_{x2}=1.6.
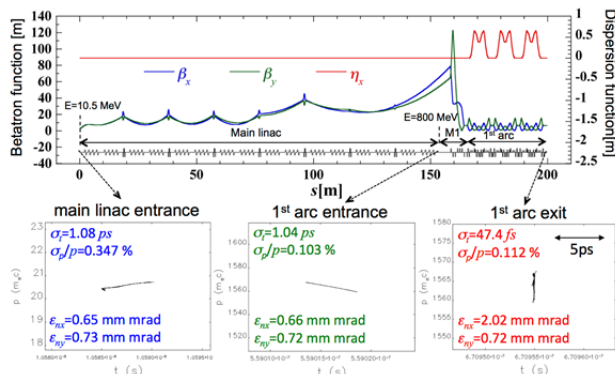

Figure 3: Betatron and dispersion functions from the main-linac entrance to the 1st arc exit (upper) and the time-momentum distributions with the basic beam parameters at the main-linac entrance, the 1st arc entrance and exit (lower).

Figure 3 shows the simulation result of the bunch compression by the simulation code *elegant* [9] for the injection beam described above. The RF phase of the main linac and the field strengths of two-family sextupole magnets (S1 and S2) are adjusted to optimize the bunch compression in the 1st arc optics. As shown in Fig. 3, the bunch is compressed to 47 fs with the energy spread of 0.112 % and the horizontal and vertical normalized emittances of 2.02 and 0.72 mm·mrad. Current and normalized horizontal and vertical slice emittances at the exit of the 1st arc are shown in Fig. 4. Thanks to the DBA optics, the peak current exceeds 700 A and the horizontal slice emittance is kept within 1.5 mm·mrad around the peak current and significantly smaller than the projected one.
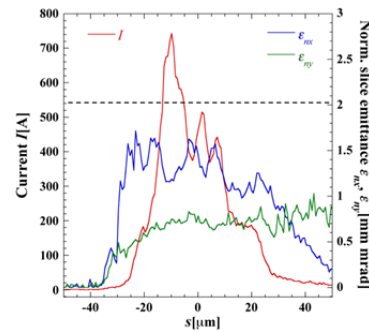

Figure 4: Current and horizontal and vertical normalized slice emittances in the bunch at the exit of the 1st arc. The broken line indicates the projected horizontal normalized emittance.

SASE FEL

The self-amplified spontaneous emission (SASE) FEL simulation is performed with the FEL simulation code *Genesis* (version 3) [10] and the electron distribution after the bunch compression. The FEL system consists of eighteen 4.9-m circular-polarizing undulator segments with the undulator period of 28 mm and the undulator K-value of 1.656 for the wavelength of 13.5 nm (the photon energy of 91.84 eV). Seventeen focusing quadrupole magnets are placed in 1.12-m gaps between each two segments and two quadrupole magnets with the half length are 5.6 m before the 1st segment and after the last segment. Quadrupole magnets are also placed in the matching section in front of the FEL system to maximize the FEL power by adjusting the Twiss parameters at the FEL entrance.

Figures 5a to 5c show results of the SASE-FEL simulation. The Twiss parameters are adjusted to β_x=14 m, β_y=14 m, $\alpha_x=\alpha_y=0$ at the FEL entrance. The FEL pulse energies without undulator tapering and with the optimum linear tapering of 2 % are shown as a function of the undulator section length in Fig. 5a. For bunch frequency of 162.5/325 MHz, the FEL power with the 2% undulator tapering reaches 14.4/28.8 kW at the average beam current of 9.75/19.5 mA. The FEL temporal profile with the electron beam current profile and the FEL spectrum are shown in Figs. 5b and 5c. The FEL spectrum is found

to be narrow compared to the reflectivity bandwidth of the Mo/Si multi-layer mirror.

The six-dimensional electron distribution just after the FEL is also produced by *Genesis* in order to proceed with the S2E simulation. Figures 6a and 6b shows the time to momentum (*t-p*) distributions at the FEL entrance and exit. As shown by comparing these figures, electrons at high currents in the bunch lose part of the energies or momenta because of the EUV-FEL lasing and as a result the averaged beam energy is slightly decreased and the energy spread is significantly increased up to ~0.3 %, while the horizontal and vertical emittances are almost unchanged.
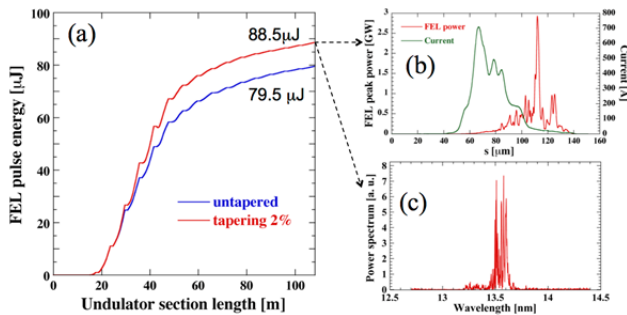

Figure 5: Results of the FEL simulation: (a) the FEL pulse energy without and with tapering as function of the undulator section length, (b) the FEL temporal profile and (c) the FEL power spectrum for 2% tapering at the FEL exit.
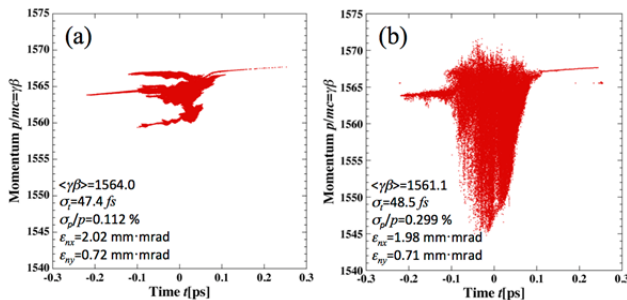

Figure 6: Time-momentum (*t-p*) distributions in the electron bunch at (a) the entrance and (b) the exit of the FEL system.

BUNCH DECOMPRESSION AND ENERGY RECOVERY

The electron bunch is decompressed in the 2nd arc after the FEL and then decelerated by the main linac in order to achieve efficient energy recovery without significant beam loss. Two TBA cells with R_{56}=-0.25 m are used as the 2nd arc for the bunch decompression. Simulation from the FEL exit to the exit of the decelerating main linac is performed by *elegant* with the six-dimensional electron distribution at the FEL exit. Figure 7 shows the betatron and dispersion functions from the FEL exit to the exit of the decelerating main linac and the time-momentum distributions with the basic beam parameters at the FEL exit, the 2nd arc exit and the exit of the decelerating main

linac. The decelerating RF phase of the main linac and the field strengths of two-family setupole magnets of the 2nd arc are adjusted to optimize the bunch decompression and the energy recovery. The beam is decelerated by the main linac to about 10.5 MeV and the momentum spread is 1.55 % for the beam energy. The bunch is finally decompressed to about 2.5 ps at the exit of the main linac and the bunch length is 2.5-times as long as that of the injection beam mainly due to the FEL lasing. The horizontal maximum beam size is 3.1 mm in the dispersion section of the 2nd arc and small enough for the assumed horizontal half-aperture of the beam pipe (35 mm). As a result the electron beam is transported to the exit of the decelerating main linac without any beam loss.
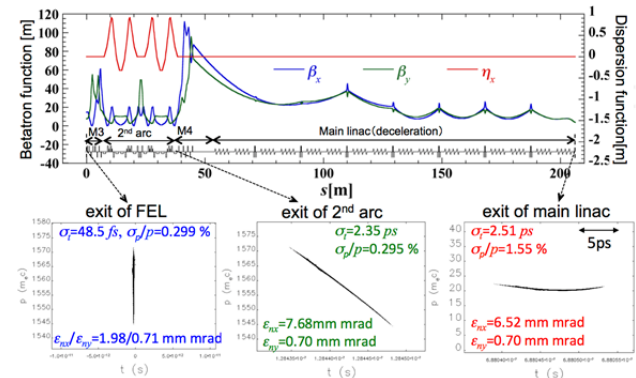

Figure 7: Betatron and dispersion functions from the FEL exit to the exit of the decelerating main linac (upper) and the time-momentum distributions with the basic beam parameters at the FEL exit, the 2nd arc exit and the exit of the decelerating main linac (lower).

CONCLUSIONS

In the S2E simulation, FEL power of higher than 10 kW is generated at the average beam current of about 10 mA in the ERL-based EUV-FEL source designed with available technologies and resources. It is also shown that the electron beam is successfully transported throughout the EUV-FEL source without any beam loss even after the FEL lasing. This result greatly enhances the feasibility of the high-power ERL-based EUV source for lithography.

REFERENCES

[1] H. Mizoguchi *et al.*, in *Proc. of SPIE 10143*, Extreme Ultraviolet (EUV) Lithography VIII, 101431J (March 27, 2017); doi:10.1117/12.2256652.

[2] E. Hosler *et al.*, in *Proc. of SPIE 9422*, Extreme Ultraviolet (EUV) Lithography VI, 94220D (March 13, 2015); doi:10.1117/12.2085538.

[3] N. Nakamura *et al.*, in *Proc. of ERL2015*, June 7-12, Stony Brook, NY, USA, pp.4-9 (2015).

[4] M. Yamamoto *et al.*, in *Proc. ERL2015*, June 7-12, Stony Brook, NY, USA, paper TUIBLH1020.

[5] E. Kako *et al.*, in *Proc. of IPAC2012*, New Orleans, LA, USA, pp.2239-2241 (2012).

[6] H. Sakai *et al.*, in *Proc. of SRF2015*, September 13-18, Whistler, BC, Canada, pp.592-596 (2015).

[7] *GPT*, http://www.pulsar.nl/gpt/index.html

[8] S. di Mitri *et al*., *Nucl. Instrum. and Methods* A 806 (2016) 184.

[9] M. Borland, "elegant: A Flexible SDDS-Compliant Code for Accelerator Simulation," Advanced Photon Source LS-287, September 2000.

[10] Genesis, http://genesis.web.psi.ch